SUPPLEMENTAL MATERIAL

Continuous Sensing and Parameter Estimation with the Boundary Time Crystal

Albert Cabot[1], Federico Carollo[1], Igor Lesanovsky[1,2,3]

[1] *Institut für Theoretische Physik, Universität Tübingen, Auf der Morgenstelle 14, 72076 Tübingen, Germany*
[2] *School of Physics and Astronomy, University of Nottingham, Nottingham, NG7 2RD, United Kingdom*
[3] *Centre for the Mathematics and Theoretical Physics of Quantum Non-Equilibrium Systems, University of Nottingham, Nottingham, NG7 2RD, United Kingdom*

CALCULATION OF THE QFI OF THE SYSTEM AND EMISSION FIELD

The QFI of the system and emission field is obtained from the joint system-and-output state. For an arbitrary measurement time T this QFI is given by [1]:

$$F_{\mathrm{E}}(g,T) = 4\partial_{g_1}\partial_{g_2}\log(|\mathrm{Tr}[\hat{\rho}_{g_1,g_2}(T)]|)\big|_{g_1=g_2=g}, \tag{S1}$$

where g is the parameter to be estimated. Here $\hat{\rho}_{g_1,g_2}(T)$ is the solution of the following deformed master equation [1, 2]:

$$\frac{d\hat{\rho}_{g_1,g_2}}{dT} = \mathcal{L}(g_1,g_2)\hat{\rho}_{g_1,g_2} \tag{S2}$$

with

$$\mathcal{L}(g_1,g_2)\hat{\rho} = -i\hat{H}(g_1)\hat{\rho} + i\hat{\rho}\hat{H}(g_2) + \hat{L}_j(g_1)\hat{\rho}\hat{L}_j^\dagger(g_2) - \frac{1}{2}\big(\hat{L}_j^\dagger(g_1)\hat{L}_j(g_1)\hat{\rho} + \hat{\rho}\hat{L}_j^\dagger(g_2)\hat{L}_j(g_2)\big) \tag{S3}$$

and initial condition $\hat{\rho}_{g_1,g_2}(0) = \hat{\rho}(0)$. The parameter g can be encoded both in the Hamiltonian and jump operators. In this work, we will focus on sensing in the stationary state. In the long time limit, the procedure to obtain the Fisher information simplifies to [1, 2]:

$$\lim_{T\to\infty}\frac{F_{\mathrm{E}}(g,T)}{T} = 4\partial_{g_1}\partial_{g_2}\mathrm{Re}[\lambda_{\mathrm{E}}(g_1,g_2)]\big|_{g_1=g_2=g} \tag{S4}$$

where $\lambda_{\mathrm{E}}(g_1,g_2)$ is the dominant eigenvalue of $\mathcal{L}(g_1,g_2)$, i.e., the one with the largest real part. As long as the stationary state is unique, for large times the Fisher information of the system and emission field increases linearly. Thus we can see the right hand side of Eq. (S4) as the rate at which this Fisher information increases with time in the asymptotic regime: i.e., the maximum possible rate at which sensitivity can be increased by increasing the measurement time.

LARGE DEVIATION APPROACH TO PHOTOCOUNTING

In this work we consider systems described by the standard Markovian master equation in Lindblad form [3]:

$$\partial_t\hat{\rho} = -i[\hat{H},\hat{\rho}] + \mathcal{D}[\hat{L}]\hat{\rho}, \tag{S5}$$

where $\hat{H}$ is the Hamiltonian of the system and $\hat{L}$ the jump operator. This master equation can be unraveled in a non-linear stochastic Schrödinger equation (SSE), that describes an ideal (unit detection efficiency) photocounting monitoring process [3]:

$$d|\Psi(t)\rangle = dN(t)\left(\frac{\hat{L}}{\sqrt{\langle\hat{L}^\dagger\hat{L}\rangle_{\mathrm{pc}}(t)}} - 1\right)|\Psi(t)\rangle + [1-dN(t)]dt\left(\frac{\langle\hat{L}^\dagger\hat{L}\rangle_{\mathrm{pc}}(t)}{2} - \frac{\hat{L}^\dagger\hat{L}}{2} - i\hat{H}\right)|\Psi(t)\rangle. \tag{S6}$$

The SSE describes the conditioned (by the measurement protocol) state of the system $|\Psi(t)\rangle$, and expected values with the subscript 'pc' are taken with this state. The quantity $dN(t)$ is a random variable taking the value one if a photon is detected at time t and zero otherwise. Its average value with respect to the instantaneous state in a trajectory is given by:

$$\mathbb{E}[dN(t)] = dt\langle \hat{L}^\dagger \hat{L}\rangle_{\rm pc}(t). \tag{S7}$$

Collecting the number of detections for a measurement time window T, we can define the emission or output intensity as

$$I_T = \frac{1}{T}\int_0^T dN(t). \tag{S8}$$

The time-integrated count record is the central quantity of our sensing protocols. In the long-time measurement limit, it approaches the emission intensity in the stationary state of the master equation:

$$\lim_{T\to\infty} \mathbb{E}[I_T] = {\rm Tr}[\hat{L}^\dagger \hat{L}\hat{\rho}_{\rm ss}] \tag{S9}$$

In the limit $T\to\infty$, the average over realizations in Eq. (S9) can be dropped out, i.e. the time-integrated quantity tends to its mean, as in a law of large numbers. The way in which this occurs can be understood within the framework of large deviations theory. This is important in our sensing approach, as it quantifies how the estimation error changes with measurement time.

In Ref. [4] a large deviation approach for open quantum systems monitored by ideal photocounting is presented. The central quantity is the partition function:

$$Z_T(s) = \mathbb{E}\big[e^{-sTI_T}\big], \tag{S10}$$

from which we can obtain the moments and cumulants of I_T as partial derivatives with respect to the conjugate field s around $s=0$. Of particular interest for us are the mean and the variance of the emitted intensity:

$$\mathbb{E}[I_T] = -\frac{1}{T}\partial_s Z_T(s)\big|_{s=0}, \tag{S11}$$

$$\mathbb{E}[I_T^2] - \mathbb{E}[I_T]^2 = \frac{1}{T^2}\partial_s^2 \log[Z_T(s)]\big|_{s=0}. \tag{S12}$$

The partition function can be calculated as $Z_T(s) = {\rm Tr}[\hat{\rho}_s(T)]$, where $\hat{\rho}_s(T)$ is the solution of the tilted master equation [4, 5]:

$$\frac{d}{dT}\hat{\rho}_s = -i[\hat{H},\hat{\rho}_s] + \mathcal{D}[\hat{L}]\hat{\rho}_s + (e^{-s}-1)\hat{L}\hat{\rho}_s\hat{L}^\dagger. \tag{S13}$$

This defines the tilted Liouvillian, $\partial_T\hat{\rho}_s = \mathcal{L}(s)\hat{\rho}_s$. This generator is not trace preserving, though it preserves positivity. Therefore, its dominant eigenvalue, denoted by $\theta(s)$, is real and generally non-zero. This eigenvalue corresponds to the (stationary) *scaled cumulant generating function*, and one can obtain all cumulants from its relation with the partition function:

$$\lim_{T\to\infty}\frac{1}{T}\log[Z_T(s)] = \theta(s). \tag{S14}$$

Thus, for large measurement times T:

$$\lim_{T\to\infty}\mathbb{E}[I_T] = -\partial_s\theta(s)|_{s=0}, \tag{S15}$$

and

$$\lim_{T\to\infty}\mathbb{E}[I_T^2] - \mathbb{E}[I_T]^2 = \frac{1}{T}\partial_s^2\theta(s)|_{s=0}. \tag{S16}$$

As $\theta(s)$ does not depend on T, in the long-time limit the variance diminishes as T^{-1}. This means that the estimation error diminishes as $\sqrt{T}$, as stated in the main text. Finally, we find that the prefactor for the estimation error can be written entirely in terms of the scaled cumulant generating function:

$$\overline{\delta\omega} = \frac{\sqrt{\theta''(0)}}{|\partial_\omega\theta'(0)|}. \tag{S17}$$

This formula combined with a Holstein-Primakoff approach can be used to obtain (approximate) analytical expressions for the estimation error in the stationary phase.

DARK STATE FOR THE CASCADED SYSTEM

In this section we show that the stationary state of the cascaded system is a dark state as long as the sensor and the decoder have the same Rabi frequency, i.e. $\omega = \omega_{\rm D}$. For a state to be a dark stationary state, it has to be an eigenstate of the Hamiltonian [6]:

$$\big[\omega\hat{S}_{\rm x}^{(1)} + \omega\hat{S}_{\rm x}^{(2)} - i\frac{\kappa}{2}(\hat{S}_{+}^{(2)}\hat{S}_{-}^{(1)} - \hat{S}_{+}^{(1)}\hat{S}_{-}^{(2)})\big]|\Psi\rangle = \varepsilon_\Psi|\Psi\rangle, \tag{S18}$$

and it has to be annihilated by the jump operator:

$$(\hat{S}_{-}^{(1)} + \hat{S}_{-}^{(2)})|\Psi\rangle = 0. \tag{S19}$$

The second condition implies that the dark state can be written in the basis of the collective angular momentum $\hat{J}_\alpha = \hat{S}_\alpha^{(1)} + \hat{S}_\alpha^{(2)}$ in terms of all states annihilated by $\hat{J}_-$. Hence, the general form for this state reads:

$$|\Psi\rangle = \sum_{J=0}^{2S} A_J|J,-J\rangle, \tag{S20}$$

where $|J,-J\rangle$ denote the collective angular momentum states with angular momentum J and z-component $-J$:

$$|J,-J\rangle = \sum_{m_1,m_2} C^{J,-J}_{S,m_1;S,m_2}|S,m_1;S,m_2\rangle. \tag{S21}$$

In the above equation $C^{J,-J}_{S,m_1;S,m_2}$ denote the Clebsch-Gordan coefficients while $|S,m_1;S,m_2\rangle$ denotes the state in which the z-component of the angular momentum of the sensor is m_1 and of the decoder is m_2.

General solution.– The state of Eq. (S20) satisfies automatically the second condition [Eq. (S19)]. The first condition [Eq. (S18)] can be satisfied for $\varepsilon_\Psi = 0$ if the coefficients $A_{\rm J}$ satisfy the following recursive relation:

$$\begin{aligned}\omega\sqrt{2J}C^{J,-J+1}_{S,m_1;S,m_2}A_J = \quad & i\kappa\Big[(1-\delta_{-S,m_1+1})(1-\delta_{S,m_2-1})P_+C^{J-1,-J+1}_{S,m_1+1;S,m_2-1} \\ & -(1-\delta_{S,m_1-1})(1-\delta_{-S,m_2+1})P_-C^{J-1,-J+1}_{S,m_1-1;S,m_2+1}\Big]A_{J-1}\end{aligned} \tag{S22}$$

with

$$P_\pm = \sqrt{(S\pm m_1+1)(S\mp m_1)(S\mp m_2+1)(S\pm m_2)}. \tag{S23}$$

The previous relation is valid for:

$$J\in[1,2S] \quad \text{and} \quad -J+1 = m_1+m_2. \tag{S24}$$

Then, the general solution reads:

$$A_{2S} = \frac{1}{\sqrt{\mathcal{N}}}, \quad A_J = \left(\frac{\omega}{i\kappa}\right)^{2S-J}\frac{a_J}{\sqrt{\mathcal{N}}}, \quad J\in[0,2S-1]. \tag{S25}$$

with the normalization constant given by:

$$\mathcal{N} = 1 + \sum_{J=0}^{2S-1}\left(\frac{\omega}{\kappa}\right)^{4S-2J}a_J^2. \tag{S26}$$

Notice that a_J are numerical constants independent of ω and κ, and only determined by S and J through Clebsch-Gordan coefficients and $P_\pm$.

In the recursive relation [Eq. (S22)] the condition $-J+1 = m_1+m_2$ can be satisfied by multiple choices of $m_{1,2}$. All these choices must give an equivalent equation for the A_J's in order for $|\Psi\rangle$ to be an eigenstate of the Hamiltonian. We do not provide an analytical proof for this equivalence. However, we have made a computer program that generates the dark state by solving this recursion relation (for a particular choice of $-J+1 = m_1+m_2$) and checks whether it is an eigenstate of the Hamiltonian with zero eigenvalue. This computer program has confirmed that this is the case for various (random) choices of N and ω/κ. Moreover, we have numerically diagonalized the master equation in the

dark state condition $\omega = \omega_{\rm D}$ for various points in parameter space, finding that it always displays a unique stationary state. Therefore, we conclude that the dark state obtained from Eqs. (S20) (S22) and (S25) is the stationary state of the system.

Benchmarking with known results. – As a first check we find that for $S = 1/2$, i.e., two spins, $a_0 = \sqrt{2}$, and thus:

$$|\Psi\rangle \propto |1,-1\rangle - i\sqrt{2}(\omega/\kappa)|0,0\rangle. \tag{S27}$$

This is the same result as found in Ref. [6] (notice a differing factor 2 due to the fact that they are defining the Hamiltonian with Pauli matrices). A second interesting scenario is that of the limits $\omega/\kappa = 0$ and $\omega/\kappa \gg 1$. In the former case $|\Psi\rangle = |2S,-2S\rangle$, i.e., all the spins are in the down state. In the latter, we obtain $|\Psi\rangle \approx |0,0\rangle$, which when tracing out the decoder yields the identity matrix for the sensor. Both of these limits coincide with what is known for the individual BTC [7].

Magnetization of each collective spin. – The dark state of Eq. (S20) has some interesting properties with regards to the individual spin expectation values. In particular, we find that:

$$\langle \hat{S}_{\rm z}^{(j)} \rangle_\Psi = \sum_{J=0}^{2S} |A_J|^2 \langle J,-J|\hat{S}_{\rm z}^{(j)}|J,-J\rangle, \tag{S28}$$

$$\langle \hat{S}_{-}^{(j)} \rangle_\Psi = \sum_{J=1}^{2S} A_J^* A_{J-1} \langle J,-J|\hat{S}_{-}^{(j)}|J-1,-J+1\rangle, \tag{S29}$$

where $\langle \dots \rangle_\Psi$ denotes an expected value taken with respect to the dark state. The first property [Eq. (S28)] comes from the fact that the application of $\hat{S}_{\rm z}^{(j)}$ does not change the value $m_1 + m_2 = -J$ and thus it does not connect different sectors of total z-component. The second property [Eq. (S29)] comes from the fact that the application of $\hat{S}_{-}^{(j)}$ changes by one the sum $m_1 + m_2$ and thus it can only give non-zero contributions when sandwiched by the state of the neighbouring sector $J+1$.

The states $|J,-J\rangle$ are either symmetric or antisymmetric with respect to the exchange of the labels 1 and 2, and hence to which is the sensor and which is the decoder. This is because of the following property of the Clebsch-Gordan coefficients:

$$C^{J,M}_{S,m_1;S,m_2} = (-1)^{J-2S} C^{J,M}_{S,m_2;S,m_1}. \tag{S30}$$

By extension, we find the following two properties:

$$C^{J,M}_{S,m_1';S,m_2'} C^{J,M}_{S,m_1;S,m_2} = (-1)^{2(J-2S)} C^{J,M}_{S,m_2';S,m_1'} C^{J,M}_{S,m_2;S,m_1}, \tag{S31}$$

and

$$C^{J,M}_{S,m_1';S,m_2'} C^{J-1,M}_{S,m_1;S,m_2} = (-1)^{2(J-2S)-1} C^{J,M}_{S,m_2';S,m_1'} C^{J-1,M}_{S,m_2;S,m_1}. \tag{S32}$$

From Eq. (S31) it follows that the matrix elements $\langle J,-J|\hat{S}_{\rm z}^{(j)}|J,-J\rangle$ are invariant under exchange of the label j. Instead, Eq. (S32) tells us that the matrix elements $\langle J,-J|\hat{S}_{-}^{(j)}|J-1,-J+1\rangle$ change sign under exchange of the label j. Therefore, going back to Eqs. (S28) and (S29) we find that:

$$\langle \hat{S}_{\rm z}^{(1)} \rangle_\Psi = \langle \hat{S}_{\rm z}^{(2)} \rangle_\Psi, \quad \langle \hat{S}_{-}^{(1)} \rangle_\Psi = -\langle \hat{S}_{-}^{(2)} \rangle_\Psi. \tag{S33}$$

Moreover, since $A_J^* A_{J-1}$ is purely imaginary [see Eq. (S25)], we obtain:

$$\langle \hat{S}_{\rm x}^{(1,2)} \rangle_\Psi = 0, \quad \langle \hat{S}_{\rm y}^{(1)} \rangle_\Psi = -\langle \hat{S}_{\rm y}^{(2)} \rangle_\Psi. \tag{S34}$$

These results allow us to apply the mean-field theory for the individual BTC to the cascaded system in the stationary phase. In particular, we know that the reduced state of the sensor is the same of the individual BTC. Thus, the mean-field approximation for $\omega/\omega_{\rm c} < 1$ yields (see e.g. [8]):

$$\langle \hat{S}_{\rm y}^{(1)} \rangle_{\rm ss} = \frac{N\omega}{2\omega_{\rm c}}, \quad \langle \hat{S}_{\rm z}^{(1)} \rangle_{\rm ss} = -\frac{N}{2}\sqrt{1 - \frac{\omega^2}{\omega_c^2}}. \tag{S35}$$

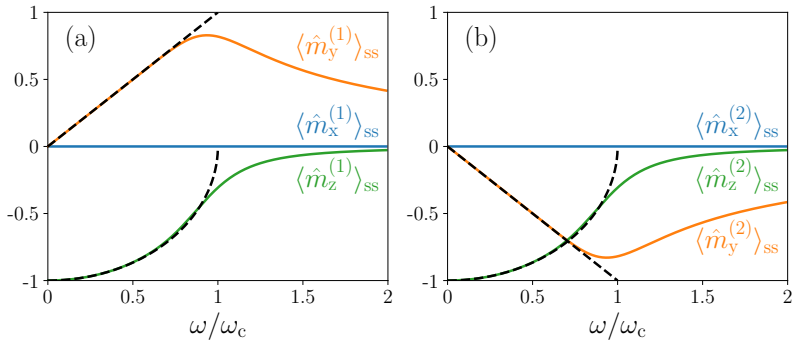

FIG. S1. **Stationary state observables for the cascaded system.** Single spin expectation values evaluated in the stationary state of the cascaded system: $\langle \hat{m}_\alpha^{(j)} \rangle_{ss} = \langle \hat{S}_\alpha^{(j)} \rangle_{ss}/S$. The parameters are fixed to the dark state condition $\omega = \omega_D$ with $N = 10$. The color lines correspond to the exact results solving the master equation. The black broken lines correspond to the mean-field prediction of Eqs. (S35) and (S36).

For the decoder, using the derived properties, we find:

$$\langle \hat{S}_y^{(2)} \rangle_{ss} = -\frac{N\omega}{2\omega_c}, \quad \langle \hat{S}_z^{(2)} \rangle_{ss} = -\frac{N}{2}\sqrt{1-\frac{\omega^2}{\omega_c^2}}. \tag{S36}$$

These results are benchmarked in Fig. S1 by solving the master equation numerically. We observe that the y-components invert while the z-ones are identical. We also find that the mean-field results are reasonably accurate given the fact that we are considering small sizes.

HOLSTEIN-PRIMAKOFF APPROACH FOR THE INDIVIDUAL SYSTEM

The main results of this section are approximate analytical expressions for the estimation error [see Eqs. (S56) and (S57)] and the QFI [see Eqs. (S78) and (S79)] in the stationary phase. Moreover, we numerically benchmark these expressions in Figs. S2 and S3, respectively, finding good agreement. In order to obtain such expressions, we make use of the Holstein-Primakoff (HP) approximation and we apply it to the calculation of dominant eigenvalue of the tilted master equation [Eq. (S13)] and of the deformed master equation [Eq. (S3)]. This approach also provides us important physical insights on the interpretation of the results, as discussed in the main text.

Holstein-Primakoff approximation

The starting point of the HP approximation is to express the spin operators in terms of a bosonic mode (see also Refs. [9, 10]):

$$\hat{S}_+ = \hat{b}^\dagger\sqrt{2S-\hat{b}^\dagger\hat{b}}, \quad \hat{S}_- = \sqrt{2S-\hat{b}^\dagger\hat{b}}\;\hat{b}. \tag{S37}$$

The bosonic mode is assumed to be in a large displaced state around which we study the fluctuations:

$$\hat{b} \to \hat{b} + \sqrt{S}\beta, \tag{S38}$$

where β is a complex field to be determined. We proceed to expand the spin operators in powers of the small parameter $\epsilon = 1/\sqrt{S}$:

$$\hat{m}_\alpha = \frac{\hat{S}_\alpha}{S} = \sum_{l=0}^{\infty} \epsilon^l \hat{m}_{\alpha,l}. \tag{S39}$$

For our purposes it is only relevant to write down the following explicit expressions:

$$m_{+,0} = \sqrt{k}\beta^*, \quad \hat{m}_{+,1} = \frac{1}{2\sqrt{k}}\left[(4-3|\beta|^2)\hat{b}^\dagger - \beta^{*2}\hat{b}\right], \tag{S40}$$

with $k = 2 - |\beta|^2$.

Before introducing these operators in the master equation and separating by orders, we need to make some physical considerations. First, since the critical point shifts with system size ($\omega_c = \kappa S$), the Rabi frequency can become an extensive parameter, and we need to account for this explicitly:

$$\omega = \tilde{\omega} S, \tag{S41}$$

where $\tilde{\omega}$ is intensive. Due to this fact, the dynamics accelerates with system size and thus time also needs to be rescaled:

$$\tau = St. \tag{S42}$$

This is essentially the same scaling of parameters prescribed in Ref. [11] for a semiclassical expansion. It is different from the one in Ref. [10] because we consider a fixed decay rate (while there it is scaled with system size).

After the rescaling we arrive to the following master equation:

$$\partial_\tau \hat{\rho} = -i\tilde{\omega} S[\hat{m}_x, \hat{\rho}] + \kappa S\big(\hat{m}_- \hat{\rho} \hat{m}_+ - \frac{1}{2}\{\hat{m}_+ \hat{m}_-, \hat{\rho}\}\big). \tag{S43}$$

We now expand the density matrix in powers of ϵ:

$$\hat{\rho} = \sum_{l=0}^{\infty} \epsilon^l \hat{\rho}_l \tag{S44}$$

where $\mathrm{Tr}[\hat{\rho}_0] = 1$ and $\mathrm{Tr}[\hat{\rho}_{l\geq 1}] = 0$. Then, we plug all the expanded operators and density matrix into the master equation and we separate order by order.

The leading order scales with $\sqrt{S}$ and it provides a self-consistent equation for β:

$$-i\tilde{\omega} \pm \kappa m_{\pm,0} = 0 \implies \beta\sqrt{2 - |\beta|^2} = -i\frac{\tilde{\omega}}{\kappa}. \tag{S45}$$

Then $m_{\pm,0} = \pm i\tilde{\omega}/\kappa$ and $\beta = -i\sqrt{1 - \sqrt{1 - (\tilde{\omega}/\kappa)^2}}$. This solution corresponds to the mean-field stable one. Notice that this is only valid in the stationary phase in which $\tilde{\omega} \leq \kappa$.

The next leading term is zero order in ϵ. This describes the leading dynamics of the bosonic fluctuations around the large displaced state. After some algebra one can write this term as a master equation for the fluctuations:

$$\partial_\tau \hat{\rho}_0 = \kappa\big(\hat{m}_{-,1} \hat{\rho}_0 \hat{m}_{+,1} - \frac{1}{2}\{\hat{m}_{+,1}\hat{m}_{-,1}, \hat{\rho}_0\}\big). \tag{S46}$$

For our purposes it is enough to consider this description for the fluctuations and we do not proceed further in the expansion. Notice that this master equation is quadratic, and thus the statistics of the fluctuations are Gaussian. The stationary state is the vacuum state of the jump operator:

$$\hat{\rho}_{0,\mathrm{ss}} = |E_0\rangle\langle E_0|, \quad \hat{m}_{-,1}|E_0\rangle = 0. \tag{S47}$$

In order to find and show that this state exists in all the stationary phase, we first rewrite more explicitly the jump operator:

$$\hat{m}_{-,1} = A\hat{b} + B\hat{b}^\dagger, \tag{S48}$$

with

$$A = \frac{1 + 3\sqrt{1 - (\tilde{\omega}/\kappa)^2}}{2\sqrt{1 + \sqrt{1 - (\tilde{\omega}/\kappa)^2}}}, \quad B = \frac{1 - \sqrt{1 - (\tilde{\omega}/\kappa)^2}}{2\sqrt{1 + \sqrt{1 - (\tilde{\omega}/\kappa)^2}}}. \tag{S49}$$

Importantly, $|B/A| \leq 1$. Then, we arrive at the following form for the stationary state:

$$|E_0\rangle = \frac{1}{\sqrt{\mathcal{N}}}|0\rangle + \frac{1}{\sqrt{\mathcal{N}}}\sum_{n=1}^{\infty}(-1)^n\left(\frac{B}{A}\right)^n\sqrt{\frac{(2n-1)!!}{2n!!}}|2n\rangle, \tag{S50}$$

where $|n\rangle$ is a Fock state and $\mathcal{N}$ is a normalization constant. This state is well defined for $\tilde{\omega} < \kappa$. It actually corresponds to a squeezed state. However, with respect to the emitted light, it appears as a vacuum state as it is annihilated by the jump operator (see also Ref. [10] for an analysis of its properties).

Calculation of the scaled cumulant generating function

The HP approximation can be combined with large deviations theory in order to obtain approximate expressions for the estimation error bound. We proceed in similar grounds as before but considering the tilted (rescaled) master equation [see Eq. (S13)]:

$$\partial_\tau \hat{\rho} = -i\tilde{\omega}S[\hat{m}_x, \hat{\rho}] + \kappa S\big(\hat{m}_-\hat{\rho}\hat{m}_+ - \frac{1}{2}\{\hat{m}_+\hat{m}_-, \hat{\rho}\}\big) + \kappa S(e^{-s}-1)\hat{m}_-\hat{\rho}\hat{m}_+. \tag{S51}$$

Our goal is to study this equation around the fixed point we have found previously and in the regime in which the fluctuation master equation is valid [Eq. (S46)]. This means that we make use of the expanded operators we have found in the previous section and we take as the initial condition the stationary state of the fluctuations $\hat{\rho}_{0,\mathrm{ss}} = |E_0\rangle\langle E_0|$. Integrating Eq. (S51) for a small time step $\Delta\tau$ and separating by orders we obtain:

$$\hat{\rho}(\Delta\tau) \approx \hat{\rho}_{0,\mathrm{ss}} + \Delta\tau\kappa S(e^{-s}-1)\big[\hat{m}_{-,0} + \epsilon\hat{m}_{-,1} + \dots\big]\hat{\rho}_{0,\mathrm{ss}}[\hat{m}_{+,0} + \epsilon\hat{m}_{+,1} + \dots\big]. \tag{S52}$$

Taking into account the properties of $\hat{\rho}_{0,\mathrm{ss}}$ we see that the leading contribution is of order S and that there is no contribution of order $\sqrt{S}$ (as the stationary state is annihilated by the jump operator). Thus, up to order 1 the fluctuation stationary state is an eigenstate of the tilted master equation. From the order S we obtain:

$$\mathrm{Tr}[\hat{\rho}(\tau)] \approx e^{\tilde{\theta}(s)\tau}, \tag{S53}$$

which provides an approximate expression for the (re-)scaled cumulant generating function

$$\tilde{\theta}(s) = S(e^{-s}-1)\frac{\tilde{\omega}^2}{\kappa} + \mathcal{O}[1]. \tag{S54}$$

Taking into account that $\tau = St$, the scaled cumulant generating function in terms of the bare parameters corresponds to:

$$\theta(s) = S\tilde{\theta}(s). \tag{S55}$$

which yields:

$$\theta(s) \approx (e^{-s}-1)\frac{\omega^2}{\kappa}. \tag{S56}$$

From this expression we can obtain the estimation error presented in the main text:

$$\overline{\delta\omega} = \frac{\sqrt{\theta''(0)}}{|\partial_\omega\theta'(0)|} \approx 0.5\sqrt{\kappa}. \tag{S57}$$

Below we numerically benchmark these expressions finding good agreement.

Finally, we present an alternative approach in order to obtain the (re-)scaled cumulant generating function. This is based on solving the eigenvalue problem for the leading eigenvalue:

$$-i\tilde{\omega}S[\hat{m}_x, \hat{R}_D] + \kappa S\big(\hat{m}_-\hat{R}_D\hat{m}_+ - \frac{1}{2}\{\hat{m}_+\hat{m}_-, \hat{R}_D\}\big) + \kappa S(e^{-s}-1)\hat{m}_-\hat{R}_D\hat{m}_+ = \tilde{\theta}(s)\hat{R}_D \tag{S58}$$

in which $\tilde{\theta}(s)$ is the largest eigenvalue and $\hat{R}_D$ the associated eigenvector. The recipe is to expand everything in terms of ϵ and consider order by order. It is important to notice that the (re-)scaled cumulant generating function can be an extensive parameter, so we expand it as follows:

$$\tilde{\theta} = S\sum_{l=0}^{\infty}\epsilon^l\tilde{\theta}_l, \quad \hat{R}_D = \sum_{l=0}^{\infty}\epsilon^l\hat{R}_{D,l}. \tag{S59}$$

where we assume $\mathrm{Tr}[\hat{R}_{D,0}] = 1$. At order S we obtain the expression for $l = 0$:

$$\tilde{\theta}_0(s) = (e^{-s}-1)\frac{\tilde{\omega}^2}{\kappa}. \tag{S60}$$

Here, we have made use of the expression of β found before. This can be seen as the contribution from the large displaced state. At order $\sqrt{S}$ the fluctuations kick in and we obtain the following equation:

$$i\tilde{\omega}(e^{-s}-1)\big(\hat{m}_{-,1}\hat{R}_{D,0}-\hat{R}_{D,0}\hat{m}_{+,1}\big)=\tilde{\theta}_1\hat{R}_{D,0}. \tag{S61}$$

Hence, $\hat{R}_{D,0}$ must be an eigenstate of the jump operator: $\hat{m}_{-,1}|E_j\rangle = E_j|E_j\rangle$. Therefore:

$$-2\tilde{\omega}(e^{-s}-1)\mathrm{Im}[E_j]|E_j\rangle\langle E_j| = \tilde{\theta}_1|E_j\rangle\langle E_j|. \tag{S62}$$

This is the general eigenvalue problem at first order. However, we are only interested in one of the solutions. Below we show that $\tilde{\theta}_1'(s=0)=0$. Given the fact that the eigenvalues E_j do not depend on s (the jump operator is independent of s), the solution corresponding to the (re-)scaled cumulant generating function for the fluctuations is:

$$\tilde{\theta}_1(s)=0, \tag{S63}$$

and $\hat{R}_{D,0}=|E_0\rangle\langle E_0|$.

In order to show that $\tilde{\theta}_1'(s=0)=0$, we recall that the stationary state allows us to compute this quantity:

$$\kappa\mathrm{Tr}[\hat{S}_+\hat{S}_-\hat{\rho}_{\mathrm{ss}}] = -\theta'(s=0). \tag{S64}$$

Expressing it as $S\kappa\mathrm{Tr}[\hat{m}_+\hat{m}_-\hat{\rho}_{\mathrm{ss}}] = -\tilde{\theta}'(s=0)$ and expanding in orders of S yields:

$$S\kappa m_{+,0}m_{-,0} = S\tilde{\theta}_0'(s=0) \tag{S65}$$

$$\sqrt{S}\kappa\mathrm{Tr}[\hat{m}_{+,1}m_{-,0}\hat{\rho}_{0,\mathrm{ss}}+m_{+,0}\hat{m}_{-,1}\hat{\rho}_{0,\mathrm{ss}}] = \sqrt{S}\tilde{\theta}_1'(s=0), \tag{S66}$$

plus higher orders that are not relevant. Taking into account that $\hat{\rho}_{0,\mathrm{ss}}$ is the vacuum state of the jump operator, we obtain that $\tilde{\theta}_1'(s=0)=0$. Therefore, to leading order in S, the eigenvalue method gives:

$$\tilde{\theta}(s) = S(e^{-s}-1)\frac{\tilde{\omega}^2}{\kappa}+\mathcal{O}[1], \tag{S67}$$

which is consistent with the method based on following the dynamics that we have used before.

Numerical benchmark. – In Fig. S2 we compare Eq. (S56) with the exact result obtained by diagonalizing the corresponding tilted master equation. In panel (a) we show it as a function of s for a fixed N and $\omega/\omega_{\mathrm{c}}$. In panel (b) we study the relative error (relative difference between exact and approximation) for different system sizes and along the stationary phase. We observe the relative error to be very small in most of the phase diagram, while it increases near the transition. The larger is the system size, the more accurate is our approximation when going closer to the phase transition. Interestingly, the order of the error in Fig. S2 (b) suggests that our approximate results hold even for higher orders in the (system size) perturbative expansion, being virtually exact for small $\omega/\omega_{\mathrm{c}}$. This can be interpreted as the collective spin system being able to imitate perfectly a coherent mode when not too close from saturation.

Calculation of the QFI

Proceeding analogously we can obtain an approximate expression for the QFI in the stationary phase. In this case we compute the dominant eigenvalue of the deformed master equation for our parameter estimation problem [see Eq. (S3)]:

$$\partial_t\hat{\rho} = -i\omega_1\hat{S}_{\mathrm{x}}\hat{\rho}+i\omega_2\hat{\rho}\hat{S}_{\mathrm{x}}+\kappa\big(\hat{S}_-\hat{\rho}\hat{S}_+-\frac{1}{2}\{\hat{S}_+\hat{S}_-,\hat{\rho}\}\big). \tag{S68}$$

As before, we make use of the rescaled parameters:

$$\partial_\tau\hat{\rho} = -i\tilde{\omega}_1S\hat{m}_{\mathrm{x}}\hat{\rho}+i\tilde{\omega}_2S\hat{\rho}\hat{m}_{\mathrm{x}}+\kappa S\big(\hat{m}_-\hat{\rho}\hat{m}_+-\frac{1}{2}\{\hat{m}_+\hat{m}_-,\hat{\rho}\}\big). \tag{S69}$$

We make the following ansatz for the dominant eigenstate of the deformed master equation:

$$\hat{\rho}_0 = |E_0^{\tilde{\omega}_1}\rangle\langle E_0^{\tilde{\omega}_2}|. \tag{S70}$$

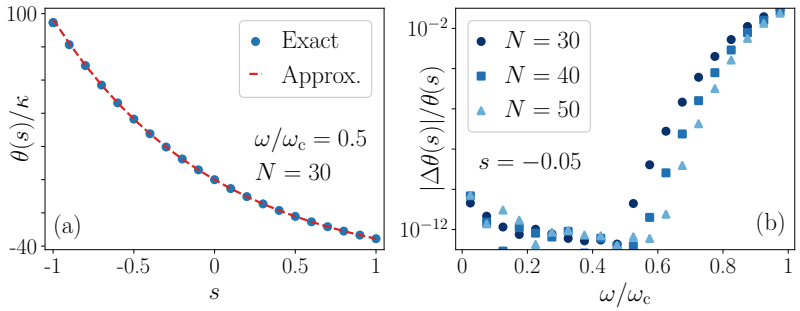

FIG. S2. **Benchmark of the approximate expression for the scaled cumulant generating function.** (a) Scaled cumulant generating function [Eq. (S14)] varying s for $\omega/\omega_c = 0.5$ and $N = 30$. The blue points are obtained diagonalizing the tilted master equation. The red dashed line corresponds to the analytical result of Eq. (S56). (b) Relative error on $\theta(s)$ as a function of ω/ω_c, for different system sizes and $s = -0.05$. This error is defined as the difference between the exact result and the analytical result of Eq. (S56), both divided by the exact result. We observe that the error increases near the transition, however, it is generally much smaller than $1/N$.

We use $|E_0^{\tilde{\omega}_j}\rangle$ to denote the stationary state of the fluctuations [Eq. (S50)] at the phase diagram point $\tilde{\omega}_j$. For the condition $\tilde{\omega}_1 = \tilde{\omega}_2 = \tilde{\omega}$ this state is the stationary state of the fluctuations. We are interested in obtaining an expression around this point, as the QFI corresponds to the curvature of this eigenvalue around it [see Eq. (S4)].

When applying the approximated spin operators to this state we must be careful, as the Bra and the Ket in Eq. (S70) describe the fluctuations at different points of the phase diagram i.e. at $\tilde{\omega}_1$ or $\tilde{\omega}_2$. This implies that, e.g.:

$$\hat{m}_-|E_0^{\tilde{\omega}_1}\rangle = \big[m_{-,0}^{\tilde{\omega}_1} + \frac{1}{\sqrt{S}}\hat{m}_{-,1}^{\tilde{\omega}_1} + \dots\big]|E_0^{\tilde{\omega}_1}\rangle, \tag{S71}$$

while

$$\langle E_0^{\tilde{\omega}_2}|\hat{m}_- = \langle E_0^{\tilde{\omega}_2}|\big[m_{-,0}^{\tilde{\omega}_2} + \frac{1}{\sqrt{S}}\hat{m}_{-,1}^{\tilde{\omega}_2} + \dots\big], \tag{S72}$$

where $\hat{m}_{-,1}^{\tilde{\omega}_j}$ denote the HP approximated operators with a β determined for the point in parameter space with $\tilde{\omega} = \tilde{\omega}_j$. Taking into account this, we can introduce our ansatz into the deformed master equation (S69) and expand order by order. Then, the right hand side of Eq. (S69) gives the following terms. The dominant term:

$$S\left[\frac{\tilde{\omega}_1\tilde{\omega}_2}{\kappa} - \frac{\tilde{\omega}_1^2 + \tilde{\omega}_2^2}{2\kappa}\right]|E_0^{\tilde{\omega}_1}\rangle\langle E_0^{\tilde{\omega}_2}|. \tag{S73}$$

The subdominant term:

$$\frac{\sqrt{S}}{2}\Big[-(i\tilde{\omega}_1 + \kappa m_{-,0}^{\tilde{\omega}_1})\hat{m}_{+,1}^{\tilde{\omega}_1}\Big]|E_0^{\tilde{\omega}_1}\rangle\langle E_0^{\tilde{\omega}_2}| + \frac{\sqrt{S}}{2}|E_0^{\tilde{\omega}_1}\rangle\langle E_0^{\tilde{\omega}_2}|\Big[(i\tilde{\omega}_2 - \kappa m_{+,0}^{\tilde{\omega}_2})\hat{m}_{-,1}^{\tilde{\omega}_2}\Big]. \tag{S74}$$

This term is zero because of the self-consistency condition [Eq. (S45)]. Notice that here we have also used that $|E_0^{\tilde{\omega}_j}\rangle$ is the vacuum state of the jump operators to first order. We do not go beyond this order. Setting the eigenvalue problem in an analogous way as for the scaled cumulant generating function, we obtain that the eigenvalue associated to $|E_0^{\tilde{\omega}_1}\rangle\langle E_0^{\tilde{\omega}_2}|$ is:

$$\tilde{\lambda}_0(\tilde{\omega}_1, \tilde{\omega}_2) = S\left[\frac{\tilde{\omega}_1\tilde{\omega}_2}{\kappa} - \frac{\tilde{\omega}_1^2 + \tilde{\omega}_2^2}{2\kappa}\right] + \mathcal{O}[1]. \tag{S75}$$

We now argue that since $|E_0^{\tilde{\omega}_1}\rangle\langle E_0^{\tilde{\omega}_2}|$ corresponds to the stationary state when $\tilde{\omega}_1 = \tilde{\omega}_2$, then very close to this point it must correspond to the dominant eigenmode of the deformed master equation [Eq. (S69)] (if the eigenspectrum is gapped, as it is the case in the stationary phase). Based on this argument we make the association:

$$\tilde{\lambda}_{\mathrm{E}}(\tilde{\omega}_1, \tilde{\omega}_2) = \tilde{\lambda}_0(\tilde{\omega}_1, \tilde{\omega}_2), \tag{S76}$$

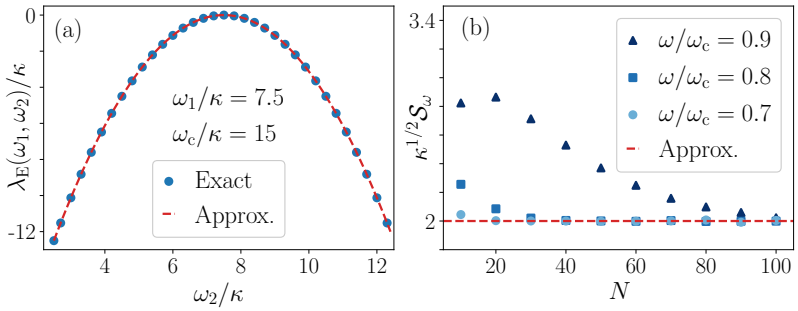

FIG. S3. **Benchmark approximate expression for the QFI.** (a) Dominant eigenvalue of the deformed master equation [Eq. (S68)] as a function of ω_2 and fixing $\omega_1/\kappa = 7.5$ (i.e. $\omega_1/\omega_c = 0.5$) and $N = 30$. The blue points are obtained diagonalizing the deformed generator. The red dashed line corresponds to the analytical result of Eq. (S78). (b) Sensitivity bound $\mathcal{S}_\omega$ [Eq. (5) of the main text] as a function of system size. The points correspond to different values of ω/ω_c close to the bifurcation. The red dashed line corresponds to the prediction derived from Eq. (S79). We observe that the closer to the phase transition we are, the larger needs to be N in order for the HP approximation to be accurate.

which allows us to obtain the QFI through Eq. (S4). Before that, however, we must reverse the scaling of time ($\tau = St$), i.e.:

$$\lambda_E(\omega_1,\omega_2) = S\tilde{\lambda}_E(\tilde{\omega}_1,\tilde{\omega}_2), \tag{S77}$$

obtaining:

$$\lambda_E(\omega_1,\omega_2) \approx \frac{\omega_1\omega_2}{\kappa} - \frac{\omega_1^2+\omega_2^2}{2\kappa}. \tag{S78}$$

Then, the QFI in the stationary phase and for long times reads [see Eq. (S4)]:

$$F_E(\omega,t) \approx \frac{4t}{\kappa}, \tag{S79}$$

as stated in the main text.

Numerical benchmark. – We numerically benchmark Eq. (S78) in Fig. S3 (a). We observe a good agreement even far from the the condition $\omega_1 = \omega_2$. Moreover, by analyzing the relative error we observe again that this is very small, suggesting that our approximations (far from the critical point) hold even for higher orders in the (system size) perturbative expansion (not shown). In Fig. S3 (b) we focus on the sensitivity bound, as derived from Eq. (S79). In this panel we illustrate that the closer one gets to the transition, the larger needs to be the system size in order for the analytical approximate results to be valid.

HOLSTEIN-PRIMAKOFF APPROACH FOR THE CASCADED SYSTEM

In this section we apply the Holstein-Primakoff to the cascaded system in order to understand its stationary phase. The main result of this section is an approximate analytical expression for the estimation error [see Eqs. (S98) and (S99)] in the stationary phase. We numerically benchmark the analytical results in Fig. S4, finding good agreement.

Holstein-Primakoff approximation

We proceed in a similar way as in the individual case. The starting point is to express the collective spin in terms of bosonic modes:

$$\hat{S}_+^{(j)} = \hat{b}_j^\dagger\sqrt{2S - \hat{b}_j^\dagger\hat{b}_j}, \quad \hat{S}_-^{(j)} = \sqrt{2S - \hat{b}_j^\dagger\hat{b}_j}\;\hat{b}_j, \tag{S80}$$

with $j = 1, 2$. The bosonic modes are assumed in a large displaced state, around which we study the fluctuations:

$$\hat{b}_j \to \hat{b}_j + \sqrt{S}\beta_j, \tag{S81}$$

where β_j is a complex field to be determined. The spin operators can be expanded in powers of the small parameter $\epsilon = 1/\sqrt{S}$:

$$\hat{m}_\alpha^{(j)} = \frac{\hat{S}_\alpha^{(j)}}{S} = \sum_{l=0}^{\infty} \epsilon^l \hat{m}_{\alpha,l}^{(j)}. \tag{S82}$$

Again, it is only relevant to write down the following explicit expressions:

$$m_{+,0}^{(j)} = \sqrt{k_j}\beta_j^*, \quad \hat{m}_{+,1}^{(j)} = \frac{1}{2\sqrt{k_j}}\big[(4-3|\beta_j|^2)\hat{b}_j^\dagger - \beta_j^{*2}\hat{b}_j\big], \tag{S83}$$

with $k_j = 2 - |\beta_j|^2$.

The expanded operators are to be used in the cascaded master equation with rescaled Rabi frequencies and time:

$$\partial_\tau \hat{\rho} = -iS\big[\tilde{\omega}\hat{m}_x^{(1)} + \tilde{\omega}_{\mathrm{D}}\hat{m}_x^{(2)}, \hat{\rho}\big] - \frac{\kappa}{2}S\big[\hat{m}_+^{(2)}\hat{m}_-^{(1)} - \hat{m}_+^{(1)}\hat{m}_-^{(2)}, \hat{\rho}\big] + \kappa S\mathcal{D}[\hat{m}_-^{(1)} + \hat{m}_-^{(2)}]\hat{\rho}. \tag{S84}$$

The dominant term of order $\sqrt{S}$ yields self-consistent equations for β_j:

$$-i\tilde{\omega} \pm \kappa m_{\pm,0}^{(1)} = 0, \quad -i\frac{\tilde{\omega}_{\mathrm{D}}}{2} \pm \kappa m_{\pm,0}^{(1)} \pm \frac{\kappa}{2} m_{\pm,0}^{(2)} = 0, \tag{S85}$$

which have as a solution

$$m_{\pm,0}^{(1)} = \pm i\frac{\tilde{\omega}}{\kappa}, \quad m_{\pm,0}^{(2)} = \mp i\frac{2\tilde{\omega} - \tilde{\omega}_{\mathrm{D}}}{\kappa}, \quad \beta_1 = -i\sqrt{1 - \sqrt{1 - \frac{\tilde{\omega}^2}{\kappa^2}}}, \quad \beta_2 = i\sqrt{1 - \sqrt{1 - \frac{(2\tilde{\omega} - \tilde{\omega}_{\mathrm{D}})^2}{\kappa^2}}}, \tag{S86}$$

valid in the range: $\tilde{\omega} \leq \kappa$, and $|2\tilde{\omega} - \tilde{\omega}_{\mathrm{D}}| \leq \kappa$. This leads to the mean-field magnetizations in the stationary state with components (the x-components are zero):

$$\langle \hat{S}_{\mathrm{y}}^{(1)} \rangle_{\mathrm{ss}} = \frac{\omega}{\kappa}, \quad \langle \hat{S}_{\mathrm{z}}^{(1)} \rangle_{\mathrm{ss}} = -\frac{N}{2}\sqrt{1 - \frac{\omega^2}{\omega_c^2}}, \quad \langle \hat{S}_{\mathrm{y}}^{(2)} \rangle_{\mathrm{ss}} = -\frac{2\omega - \omega_{\mathrm{D}}}{\kappa}, \quad \langle \hat{S}_{\mathrm{z}}^{(2)} \rangle_{\mathrm{ss}} = -\frac{N}{2}\sqrt{1 - \frac{(2\omega - \omega_{\mathrm{D}})^2}{\omega_c^2}}. \tag{S87}$$

The next leading term is a zero order term in ϵ. This describes the leading dynamics of the fluctuations:

$$\partial_\tau \hat{\rho}_0 = -\frac{\kappa}{2}\big[\hat{m}_{+,1}^{(2)}\hat{m}_{-,1}^{(1)} - \hat{m}_{+,1}^{(1)}\hat{m}_{-,1}^{(2)}, \hat{\rho}_0\big] + \kappa\mathcal{D}[\hat{m}_{-,1}^{(1)} + \hat{m}_{-,1}^{(2)}]\hat{\rho}_0. \tag{S88}$$

The stationary state for the fluctuations is the product state of vacuum states of each $\hat{m}_{-,1}^{(j)}$:

$$\hat{\rho}_{0,\mathrm{ss}} = \big(|E_0^{(1)}\rangle \otimes |E_0^{(2)}\rangle\big)\big(\langle E_0^{(1)}| \otimes \langle E_0^{(2)}|\big), \quad \hat{m}_{-,1}^{(1)}|E_0^{(1)}\rangle = 0 \quad \hat{m}_{-,1}^{(2)}|E_0^{(2)}\rangle = 0. \tag{S89}$$

The jump operators can be rewritten as:

$$\hat{m}_{-,1}^{(j)} = A_j\hat{b}_j + B_j\hat{b}_j^\dagger, \tag{S90}$$

with $A_1 = A$ and $B_1 = B$ and:

$$A_2 = \frac{1 + 3\sqrt{1 - (2\tilde{\omega} - \tilde{\omega}_{\mathrm{D}})^2/\kappa^2}}{2\sqrt{1 + \sqrt{1 - (2\tilde{\omega} - \tilde{\omega}_{\mathrm{D}})^2/\kappa^2}}}, \quad B_2 = \frac{1 - \sqrt{1 - (2\tilde{\omega} - \tilde{\omega}_{\mathrm{D}})^2/\kappa^2}}{2\sqrt{1 + \sqrt{1 - (2\tilde{\omega} - \tilde{\omega}_{\mathrm{D}})^2/\kappa^2}}}. \tag{S91}$$

These coefficients satisfy that $|B_j/A_j| \leq 1$ in the valid parameter regime. Then, the following state always exist in the stationary phase and makes up the vacuum state of the collective jump operator:

$$|E_0^{(j)}\rangle = \frac{1}{\sqrt{\mathcal{N}_j}}|0\rangle_j + \frac{1}{\sqrt{\mathcal{N}_j}}\sum_{n=1}^{\infty}(-1)^n\left(\frac{B_j}{A_j}\right)^n\sqrt{\frac{(2n-1)!!}{2n!!}}|2n\rangle_j, \tag{S92}$$

where $|n\rangle_j$ is a Fock state of boson j and $\mathcal{N}_j$ is a normalization constant. This state has analogous properties as the one for the individual system.

Calculation of the scaled cumulant generating function

The starting point is the tilted (rescaled) master equation for the cascaded system:

$$\partial_\tau \hat{\rho} = -iS\big[\tilde{\omega}\hat{m}_x^{(1)} + \tilde{\omega}_{\rm D}\hat{m}_x^{(2)}, \hat{\rho}\big] - \frac{\kappa}{2}S\big[\hat{m}_+^{(2)}\hat{m}_-^{(1)} - \hat{m}_+^{(1)}\hat{m}_-^{(2)}, \hat{\rho}\big] + \kappa S\mathcal{D}[\hat{m}_-^{(1)} + \hat{m}_-^{(2)}]\hat{\rho} \\ +\kappa S(e^{-s}-1)(\hat{m}_-^{(1)} + \hat{m}_-^{(2)})\hat{\rho}(\hat{m}_+^{(1)} + \hat{m}_+^{(2)}). \tag{S93}$$

We analyze this equation around the fixed point we have found previously and in the regime in which the fluctuation dynamics is well described by the fluctuation operators of order $l = 1$. Therefore, we plug in the fluctuation stationary state and the operators expanded up to this order in the tilted master equation. Integrating it for a small time step $\Delta\tau$ we obtain:

$$\hat{\rho}(\Delta\tau) \approx \hat{\rho}_{0,\rm ss} + \Delta\tau\kappa S(e^{-s}-1)\big[m_{-,0}^{(1)} + m_{-,0}^{(2)} + \epsilon\hat{m}_{-,1}^{(1)} + \epsilon\hat{m}_{-,1}^{(2)} + \dots\big]\hat{\rho}_{0,\rm ss}[m_{+,0}^{(1)} + m_{+,0}^{(2)} + \epsilon\hat{m}_{+,1}^{(1)} + \epsilon\hat{m}_{+,1}^{(2)}\dots]. \tag{S94}$$

Similarly to the individual system, the properties of $\hat{\rho}_{0,\rm ss}$ ensure that the leading contribution is of order S and that there is no contribution of order $\sqrt{S}$ (as the stationary state is annihilated by the jump operator). Thus, up to order 1 the fluctuation stationary state is an eigenstate of the tilted master equation and we see that:

$$\mathrm{Tr}[\hat{\rho}(\tau)] \approx e^{\tilde{\theta}_c(s)\tau}, \tag{S95}$$

where

$$\tilde{\theta}_c(s) = S(e^{-s}-1)\frac{(\tilde{\omega}-\tilde{\omega}_{\rm D})^2}{\kappa} + \mathcal{O}[1], \tag{S96}$$

is the (re-)scaled cumulant generating function. Taking into account that $\tau = St$, the scaled cumulant generating function for the bare time is related to the one for the rescaled time as:

$$\theta_c(s) = S\tilde{\theta}_c(s). \tag{S97}$$

Thus, up to leading order we obtain:

$$\theta_c(s) \approx (e^{-s}-1)\frac{(\omega-\omega_{\rm D})^2}{\kappa}. \tag{S98}$$

Using the results of the Large deviations theory we obtain the estimation error presented in the main text:

$$\overline{\delta\omega} = \frac{\sqrt{\theta_{\rm c}''(0)}}{|\partial_\omega\theta_{\rm c}'(0)|} \approx 0.5\sqrt{\kappa}. \tag{S99}$$

Numerical benchmark. – In Fig. S4, we compare the analytic approximation [Eq. (S98)] with the result obtained numerically diagonalizing tilted master equation. We find good agreement, though errors are larger than in the individual case. We observe that the relative error [Fig. S4 (b)] increases near the transition, however it is still generally smaller than $1/N$.

SEPARATION OF TIMESCALES BETWEEN COLLECTIVE AND LOCAL PROCESSES

Here we discuss the separation of timescales between the collective time-crystal oscillations and possible local decay channels. For large atom numbers and the system in the time-crystal phase, the oscillations display a dominant frequency close to the mean-field one: $\Omega \approx \frac{N\kappa}{2}\sqrt{(\omega/\omega_{\rm c})^2 - 1}$ [7, 11]. We now assume that besides collective dissipation there are also moderate local dissipation and dephasing processes occurring with a rate $\gamma_{\rm loc}$. The characteristic timescale associated to these processes is $T_{\rm loc} = \gamma_{\rm loc}^{-1}$. On the other hand, the characteristic timescale associated to the collective oscillations is their period: $T_{\rm osc} = 2\pi/\Omega \sim N^{-1}$. For large enough atom numbers we have $T_{\rm osc} \ll T_{\rm loc}$, i.e., a large separation of timescales. This means that, when initially preparing the ensemble in a fully symmetric state (e.g. all atoms excited), many time-crystal oscillations will occur before the effects of local dissipation are significant. These local incoherent terms break the conservation of total angular momentum and we expect the system to reach a different stationary state [12]. However, when $T_{\rm osc} \ll T_{\rm loc}$, we expect the time-crystal oscillations to manifest as a metastable phenomenon [13–15] in which the characteristic separation of timescales increases with atom number.

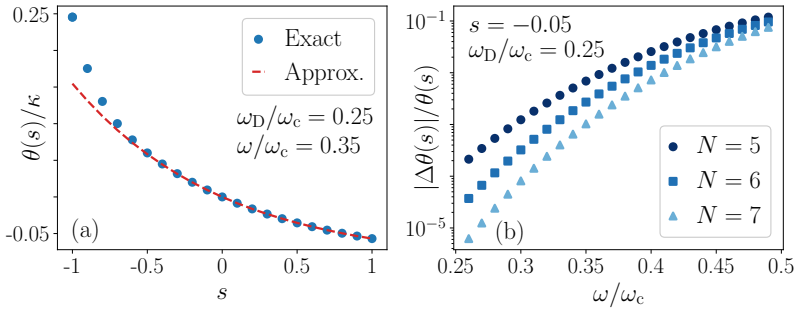

FIG. S4. **Benchmark for the scaled cumulant generating function in the cascaded system.** (a) Scaled cumulant generating function [Eq. (S14)] varying s for $\omega/\omega_c = 0.35$, $\omega_D/\omega_c = 0.25$ and $N = 6$. The blue points are obtained diagonalizing the tilted master equation. The red dashed line corresponds to the analytical result of Eq. (S98). (b) Relative error on $\theta(s)$ as a function of ω/ω_c, for different system sizes, $\omega_D/\omega_c = 0.25$ and $s = -0.05$. This error is defined as the difference between the exact result and the analytical result of Eq. (S56), both divided by the exact result.

ERROR BARS OF THE MONTECARLO RESULTS FOR THE CASCADED SYSTEM

In the study of the sensitivity for the cascaded system, we have used quantum trajectories to evaluate the estimation error for large system sizes. In this regard, we distinguish between three subsets of data:

- For $N \leq 11$, both the prefactor of the standard deviation of the intensity, $\overline{\sigma_{I_T}} = \sqrt{(\mathbb{E}[I_T^2] - \mathbb{E}[I_T]^2)T}$, and the derivative of the intensity, $\partial_\omega I_T$, have been obtained from eigenvalue methods. These consist on finding the largest eigenvalue of the tilted master equation or finding the stationary state of the master equation and performing a numerical derivative, respectively.

- For $11 < N \leq 22$, $\overline{\sigma_{I_T}}$ has been obtained from Montecarlo sampling of quantum trajectories, while $\partial_\omega I_T$ from eigenvalue methods.

- For $N > 22$, only Monte Carlo sampling of quantum trajectories is available due to its more favourable scaling in computational cost. In this case, both quantities have been obtained from quantum trajectories.

In Fig. 4 (d) of the main text, we have introduced error bars in order to account for errors associated to the Montecarlo methods. We account for different source of errors: (i) Montecarlo error due to finite sampling; (ii) systematic errors due to finite measurement time runs and effect of initial conditions. For system sizes in the range $11 < N \leq 22$, we have used samples of 10^5 trajectories per point. For system sizes in the range $N > 22$, we have used larger samples of $5 \cdot 10^5$ trajectories. This is because in order to perform the numerical derivative of $\partial_\omega I_T$ the quantity I_T needs to be determined with high precision (a step $\kappa d\omega = 0.00025$ is used to ensure enough precision in the numerical derivative). In both cases, quantum trajectories are computed for a total measurement time $\kappa T = 440$. Simulations are performed such that data is started to be compiled after $\kappa t = 40$, in order to minimize the effects of initial conditions. Then, we write the standard deviation on the estimation error as (error propagation formula):

$$\mathrm{Err}\left[\overline{\delta\omega}\right] \approx \frac{\mathrm{Err}\left[(\mathbb{E}[I_T^2] - \mathbb{E}[I_T]^2)T\right]}{2\overline{\sigma_{I_T}}|\partial_\omega I_T|} + \frac{\overline{\sigma_{I_T}}}{|\partial_\omega I_T|^2}\mathrm{Err}\left[|\partial_\omega I_T|\right]. \tag{S100}$$

Comparing Montecarlo results with the ones obtained from eigenvalue methods (for sizes in which it is possible to do so), we observe errors of the order of $1 - 2\%$ in $(\mathbb{E}[I_T^2] - \mathbb{E}[I_T]^2)T$ and errors of the order of 5% in $\partial_\omega I_T$. We thus make the estimation that $\mathrm{Err}[(\mathbb{E}[I_T^2] - \mathbb{E}[I_T]^2)T] \sim 0.02(\mathbb{E}[I_T^2] - \mathbb{E}[I_T]^2)T$ and $\mathrm{Err}[|\partial_\omega I_T|] \sim 0.05|\partial_\omega I_T|$.

[1] S. Gammelmark and K. Mølmer, Phys. Rev. Lett. **112**, 170401 (2014).
[2] K. Macieszczak, M. Guţă, I. Lesanovsky, and J. P. Garrahan, Phys. Rev. A **93**, 022103 (2016).
[3] H. M. Wiseman and G. J. Milburn, *Quantum measurement and control* (Cambridge university press, 2009).
[4] J. P. Garrahan and I. Lesanovsky, Phys. Rev. Lett. **104**, 160601 (2010).
[5] F. Carollo, J. P. Garrahan, I. Lesanovsky, and C. Pérez-Espigares, Phys. Rev. A **98**, 010103 (2018).

[6] K. Stannigel, P. Rabl, and P. Zoller, New J. Phys. **14**, 063014 (2012).
[7] A. Cabot, L. S. Muhle, F. Carollo, and I. Lesanovsky, Phys. Rev. A **108**, L041303 (2023).
[8] F. Carollo and I. Lesanovsky, Phys. Rev. A **105**, L040202 (2022).
[9] E. M. Kessler, G. Giedke, A. Imamoglu, S. F. Yelin, M. D. Lukin, and J. I. Cirac, Phys. Rev. A **86**, 012116 (2012).
[10] V. P. Pavlov, D. Porras, and P. A. Ivanov, Physica Scripta **98**, 095103 (2023).
[11] H. J. Carmichael, J. Phys. B At. Mol. Opt. **13**, 3551 (1980).
[12] G. Piccitto, M. Wauters, F. Nori, and N. Shammah, Phys. Rev. B **104**, 014307 (2021).
[13] K. Macieszczak, M. Guţă, I. Lesanovsky, and J. P. Garrahan, Phys. Rev. Lett. **116**, 240404 (2016).
[14] B. Zhu, J. Marino, N. Y. Yao, M. D. Lukin, and E. A. Demler, New J. Phys. **21**, 073028 (2019).
[15] A. Cabot, F. Carollo, and I. Lesanovsky, Phys. Rev. B **106**, 134311 (2022).